5-2013

Compressed Sensing for Multiple Input-Multiple Output Radar Imaging

Juan F. Lopez Jr.
University of Texas-Pan American

COMPRESSED SENSING FOR MULTIPLE INPUT-MULTIPLE OUTPUT RADAR IMAGING

A Thesis

by

JUAN F. LOPEZ JR.

Submitted to the Graduate School of the
University of Texas-Pan American
In partial fulfillment of the requirements for the degree of

MASTER OF SCIENCE

May 2013

Major Subject: Mathematical Science

COMPRESSED SENSING FOR MULTIPLE INPUT-MULTIPLE OUTPUT RADAR IMAGING

A Thesis
by
JUAN F. LOPEZ JR.

COMMITTEE MEMBERS

Dr. Zhijun Qiao
Chair of Committee

Dr. Andras Balogh
Committee Member

Dr. Karen Yagdjian
Committee Member

Dr. Zhaosheng Feng
Committee Member

May 2013

ABSTRACT

Lopez, Juan F., Jr., Compressed Sensing for Multiple Input - Multiple Output Radar Imaging. Master of Science (MS), May, 2013, 33 pp., 8 figures, references, 22 titles.

Multiple input - multiple output (MIMO) radar utilizes the transmission of spatially diverse waveforms from a static antenna array to gather information about the desired scene. We will demonstrate how techniques from compressed sensing can be applied to image formation in MIMO radar when in the presence of undersampling. We analyze the problem under the general theoretical framework of inverse scattering.

DEDICATION

I would like to dedicate this thesis to my family for their unconditional love and support.

ACKNOWLEDGMENTS

I am grateful to my advisor Dr. Zhijun Qiao for his constant support and advice during the writing of this thesis. This work was partially supported by the US Department of Defense Army Research Office under grant number W911NF-08-1-0511, the Norman Hackerman Advanced Research Program under grant number 003599- 0001-2009, and the U.S. Department of Education UTPA-MATH GAANN program under grant number P200A120256.

TABLE OF CONTENTS

LIST OF FIGURES

I

INTRODUCTION

Radar is an acronym that stands for Radio Detection and Ranging. It is a remote sensing technology that uses electromagnetic radiation in the radio or microwave spectrum to detect objects over large distances. From its name, it should be clear that a true radar system must be able to both detect a target and determine its distance from the radar antenna. However, modern systems have a number of other added capabilities. For example, some radar systems are able to measure the velocity of a target in terms of the doppler-shift induced by the motion of the target, which may be either linear or rotational. Another very important application of radar is the production of high resolution images.

Multiple input - multiple output radar utilizes the transmission of multiple waveforms from spatially diverse antennas to gather information about the desired scene [18]. Specifically, the knowledge of the reflected waves are measured and the scene is by determined by the knowledge of the incident and reflected waves. Hence, the imaging problem can be cast as an inverse scattering problem.

The inverse scattering problem is then discretized to form a linear system. Solving this linear system yields the scene vector which is used to paint an approximation of the desired scene. However, this system is typically overdetermined as the dimension of the data usually exceeds the dimension of the discretized scene and various algorithms such as least squares minimization are used to obtain an approximate solution.

The advent of compressed sensing in signal processing has enabled high accurate recovery of signals when in the presence of undersampling [2]. The main requirement is that the signal needs to be sparse. In the context of MIMO radar imaging, undersampling yields an underdetermined linear system, i.e. the dimension of the data is much less than the dimension of the scene vector.

The purpose of this thesis is to study the use of compressed sensing (CS) algorithms applied to MIMO radar image formation. In particular we study the use of CS algorithms in reconstructing scenes with small targets and scenes that can be approximated with piecewise constant objects. The sensing matrix consisting of array parameters plays a crucial role in the success of these algorithms and we will analyze, by virtue of numerical simulations, the role of these parameters in the success of CS algorithms.

I.1 Thesis Chapter Outline

Here a basic outline of the thesis chapters is presented.

II:

The MIMO radar imaging problem problem is introduced. We consider the one dimensional imaging problem when the targets lie at a known range and compare particular compressed sensing techniques with other signal processing.

III:

We develop a mathematical model for the two dimensional imaging problem as an inverse scattering problem and present the compressed sensing signal processing techniques we will apply.

IV:

We illustrate the success of compressed sensing signal processing for MIMO radar imaging in the case of small, pointlike targets and extended two dimensional targets.

II

INTRODUCTION TO MIMO RADAR AND COMPRESSED SENSING

II.1 Multiple Input - Multiple Output (MIMO) Radar

The traditional problem of radar imaging concerns the remote detection of an object from the reflected data of a probing signal. Multiple input-multiple output (MIMO) radar systems utilize multiple antennas transmitting diverse waveforms to acquire information about the desired target scene. Here we introduce the concept by discussing the 1-dimensional cross range imaging problem. In cross range imaging the targets and antenna array are coplanar and the targets lie at a fixed known range away from the antenna array. Also the static transmitting antennas are colinear and serve as receiving antennas as well. We also make the simplifying assumption that the targets are pointlike. The problem then consists of estimating the cross range location of targets with nonzero reflectivity and the relative strength of the reflecting targets.

II.2 MIMO Signal Model

Let $x_\ell(t)$ denote baseband the time domain signal transmitted by the ℓth transmit antenna. The ℓth transmit antenna transmits a frequency modulated form of $x_\ell(t)$ with carrier frequency f_0, so the transmitted probing signal from the ℓth antenna has the form

$$s_\ell(t) = e^{2\pi i f_0 t} x_\ell(t). \tag{II.1}$$

Let $d_j(t)$ denote the received signal data at antenna j. We discretize the cross range space into N_k targets and let $\beta_k \in \mathbf{C}$ denote the reflectivity of a point target located at position $z_k, k = 1, \ldots, N_k$. The received signal at antenna j is the superposition of the attenuated, time delayed transmitted signals. If N_t and N_k denote the number of transmit antennas and the number of targets

respectively then the received data $d_j(t)$ has the form [18]

$$d_j(t) = \sum_{k=1}^{N_k} \sum_{\ell=1}^{N_t} \beta_k e^{-2\pi i f_0 \tau_\ell^k} e^{-2\pi i f_0 \tilde{\tau}_j^k} x_\ell(t - \tau_\ell^k - \tilde{\tau}_j^k) \tag{II.2}$$

where

$$\tau_\ell^k = \frac{|p_l - z_k|}{c_0} \tag{II.3}$$

$$\tilde{\tau}_j^k = \frac{|\tilde{p}_j - z_k|}{c_0} \tag{II.4}$$

and $p_\ell, \tilde{p}_j$ are the locations of the ℓth transmit and jth receive antennas respectively, c_0 is the speed of signal propagation. We assume the baseband signal x_ℓ is *slowly varying* for all ℓ in the sense that

$$x_\ell(t - \tau) \approx x_\ell(t) \tag{II.5}$$

when τ is small. In our model $c_0 = 3 \times 10^8$ m/s so $\tau_\ell^k, \tilde{\tau}_j^k$ are small, therefore we can apply this approximation in II.2 to get

$$d_j(t) \approx \sum_{k=1}^{N_k} \sum_{\ell=1}^{N_t} \beta_k e^{-2\pi i f_0 \tau_\ell^k} e^{-2\pi i f_0 \tilde{\tau}_j^k} x_\ell(t). \tag{II.6}$$

Henceforth, we shall write this as an equality without confusion, i.e.

$$d_j(t) = \sum_{k=1}^{N_k} \sum_{\ell=1}^{N_t} \beta_k e^{-2\pi i f_0 \tau_\ell^k} e^{-2\pi i f_0 \tilde{\tau}_j^k} x_\ell(t). \tag{II.7}$$

Set

$$\mathbf{x}(t) = (x_1(t), \ldots, x_{N_t}(t))^T \in \mathbf{C}_{N_t \times 1}, \tag{II.8}$$

$$\mathbf{a}_k = \left(e^{2\pi i f_0 \tau_1^k}, \ldots, e^{2\pi i f_0 \tau_{N_t}^k}\right)^T \in \mathbf{C}_{N_t \times 1}, \quad k = 1, \ldots, N_k, \tag{II.9}$$

$$\mathbf{b}_k = \left(e^{2\pi i f_0 \tilde{\tau}_1^k}, \ldots, e^{2\pi i f_0 \tilde{\tau}_{N_r}^k}\right)^T \in \mathbf{C}_{N_r \times 1} \quad k = 1, \ldots, N_k. \tag{II.10}$$

Then the total data received at time t has the form

$$\mathbf{d}(t) = \sum_{k=1}^{N_k} \beta_k \bar{\mathbf{b}}_k \mathbf{a}_k^* \mathbf{x}(t) \tag{II.11}$$

where

$$\mathbf{d}(t) = (d_1(t), \ldots, d_{N_r}(t))^T \in \mathbf{C}_{N_r \times 1}. \tag{II.12}$$

We write the totality of the data over all time samples $\{t_1, \ldots, t_N\}$ in matrix form as

$$\mathbf{D} = (\mathbf{d}(t_1) | \cdots | \mathbf{d}(t_N)) \in \mathbf{C}_{N_r \times N} \tag{II.13}$$

and then

$$\mathbf{D} = \bar{\mathbf{b}}_k \beta_k \mathbf{a}_k^* \mathbf{X} \tag{II.14}$$

where

$$\mathbf{X} = (\mathbf{x}(t_1) | \cdots | \mathbf{x}(t_N)) \in \mathbf{C}_{N_t \times N}. \tag{II.15}$$

The matrix equation (II.14) is the form of data used in [18] for signal processing. We will write (II.14) as an equivalent linear system to apply other signal processing techniques. Let $\mathbf{d}_j$ be the total data collected at receiver j,

$$\mathbf{d}_j = (d_j(t_1), \ldots, d_j(t_N))^T \in \mathbf{C}_{N \times 1}, \tag{II.16}$$

and for each j, define $\phi_j \in \mathbf{C}_{N \times N_k}$ as

$$\phi_j = \left(e^{-2\pi i f_0 \tilde{\tau}_j^1} \mathbf{X}^T \bar{\mathbf{a}}_k, \ldots, e^{-2\pi i f_0 \tilde{\tau}_j^{N_k}} \mathbf{X}^T \bar{\mathbf{a}}_k \right). \tag{II.17}$$

Then

$$\mathbf{d}_j = \phi_j \beta \tag{II.18}$$

where $\beta = (\beta_1, \ldots, \beta_{N_k})^T \in \mathbf{C}_{N_k \times 1}$ is the scene vector. Stacking the $\mathbf{d}_j, \phi_j$ yields the linear system

$$\mathbf{d} = \Phi\beta \tag{II.19}$$

where

$$\mathbf{d} = \begin{pmatrix} \mathbf{d}_1 \\ \vdots \\ \mathbf{d}_{N_r} \end{pmatrix} \in \mathbf{C}_{N_r N \times 1} \tag{II.20}$$

and

$$\Phi = \begin{pmatrix} \phi_1 \\ \vdots \\ \phi_{N_r \cdot} \end{pmatrix} \in \mathbf{C}_{N_r N \times N_k} \tag{II.21}$$

II.3 MIMO Signal Processing

We will consider the case of undersampling so that the dimension of the data is less than the dimension of the target vector β, i.e. $N_r N \ll N_k$. We will also suppose that received data is corrupted by complex zero mean Gaussian noise of unit variance. Li and Stoica demonstrated in [18] the success of least squares, CAPON, and APES signal processing in the case of oversampling. The least squares estimate is given by

$$(\hat{\beta}_{LS})_k = \frac{\mathbf{b}_k^T \mathbf{D}\mathbf{X}^* \mathbf{a}_k}{N \|\mathbf{b}_k\|^2 [\mathbf{a}_k^* \mathbf{R}_{xx} \mathbf{a}_k]} \tag{II.22}$$

where

$$\mathbf{R}_{xx} = \frac{1}{N}\mathbf{X}\mathbf{X}^*. \tag{II.23}$$

The CAPON and APES estimators are given, respectively, by

$$(\hat{\beta}_{Cap})_k = \frac{\mathbf{b}_k^T \mathbf{R}_{dd}^{-1} \mathbf{D}\mathbf{X}^* \mathbf{a}_k}{N [\mathbf{b}_k^T \mathbf{R}_{dd}^{-1} \bar{\mathbf{b}}_k][\mathbf{a}_k^* \mathbf{R}_{xx} \mathbf{a}_k]} \tag{II.24}$$

and

$$(\hat{\beta}_{Apes})_k = \frac{\mathbf{b}_k^T \mathbf{Q}_k^{-1} \mathbf{D}\mathbf{X}^* \mathbf{a}_k}{N[\mathbf{b}_k^T \mathbf{Q}_k^{-1} \bar{\mathbf{b}}_k][\mathbf{a}_k^* \mathbf{R}_{xx} \mathbf{a}_k]} \tag{II.25}$$

where

$$\mathbf{R}_{dd} = \frac{1}{N}\mathbf{D}\mathbf{D}^* \tag{II.26}$$

and

$$\mathbf{Q}_k = \mathbf{R}_{dd} - \frac{\mathbf{D}\mathbf{X}^* \mathbf{a}_k \mathbf{a}_k^* \mathbf{X}\mathbf{D}^*}{N^2 \mathbf{a}_k^* \mathbf{R}_{xx} \mathbf{a}_k}. \tag{II.27}$$

Candes et.al. [2] showed the effectiveness of optimization for solving linear systems when the target vector is known to be sparse, that is, has few nonzero entries and in the case of undersampling. Intuitively, if the target vector β is sparse, then all of the information in β is contained in only a few entries so sampling exceeding the dimension of β is unnecessary. To be precise, a vector v is called s-sparse if it has at most s nonzero entries. The reflecting targets in β determine the support of β and β is sparse in the present case since the targets are pointlike. In [2] it is shown that β can be recovered with overwhelming accuracy via the constrained optimization problem

$$\min \|\beta\|_1 \quad \text{s.t} \quad \mathbf{d} = \Phi\beta \tag{II.28}$$

in the absence of noise. Here $\|\cdot\|_1$ is the ℓ^1 norm

$$\|v\|_1 = \sum_i |v_i|. \tag{II.29}$$

The problem II.28 is called **basis pursuit** (BP). In the case of noisy data, we solve **basis pursuit denoising** (BPDN) [6]

$$\min \|\beta\|_1 \quad \text{s.t} \quad \|\Phi\beta - \mathbf{d}\|_2 \leq \epsilon \tag{II.30}$$

where $\epsilon > 0$ is a user parameter and $\|\cdot\|_2$ is the ℓ^2 norm

$$\|v\|_2 = \sqrt{\sum_i |v_i|^2}. \tag{II.31}$$

II.4 Simulation

The MATLAB code for this simulation is given in Appendix A. For the following simulations 10 antennas were distributed randomly along a line through the origin and white Gaussian noise modulated with carrier frequency 900 MHz was used as the transmitted baseband signal. The targets are located at a known range of 500 m and the discrete cross range space ranges from -500 m to 500 m at 5 m increments. There are 13 reflecting targets with $\beta_k = 10$ for each target. Here 16 time samples are collected. The data has dimension 160 and beta has dimension 201. The vertical lines indicate the target positions. The results are shown in figure II.1. We have used the MATLAB implementation of basis pursuit denoising by Friedlander and van den Berg [21, 20]. A picture of the scene can be inferred from the peaks in the recovered β. The data is complex valued so each signal processing technique gives a vector with complex entries, hence we plot the *modulus* of each entry.

The signal processing done with basis pursuit denoising yields a very accurate image while the images produced by least squares, CAPON, and APES are inaccurate due to undersampling. We further investigate the robustness of by increasing the strength of the measurement noise. Figure II.2 shows the results with complex Gaussian noise having mean $\nu(1 + i)$ for $\nu = 1, 3, 5, 10$. All other parameters are the same as in the previous simulation.

The higher noise levels yield noisier images, with small peaks blurring out the true locations of the targets. However, the significant peaks of the reconstructed β still correspond to the actual locations of the targets.

II.5 Conclusion

We have illustrated the superiority of BPDN in signal processing for MIMO radar imaging in the cross range with undersampling. Least squares, CAPON, and APES fail to accurately reconstruct the target vector while BPDN accurately reconstructs the desired scene even with stronger noise levels. This result is limited to the one dimensional case, but in the following chapters we present a framework to apply compressed sensing techniques for two dimensional imaging.

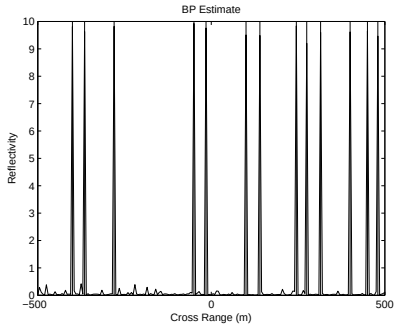

(a) Basis Pursuit Denoising

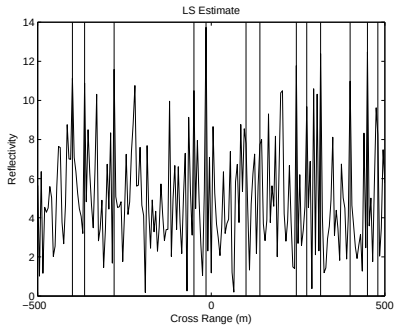

(b) Least Squares

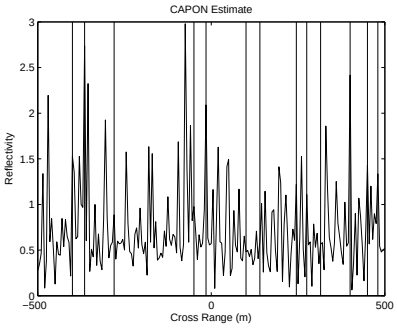

(c) CAPON

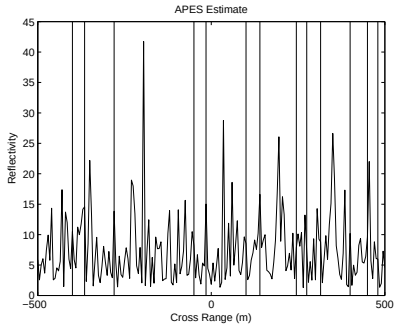

(d) APES

Figure II.1: Cross range simulation with 10 antennas and 13 targets.

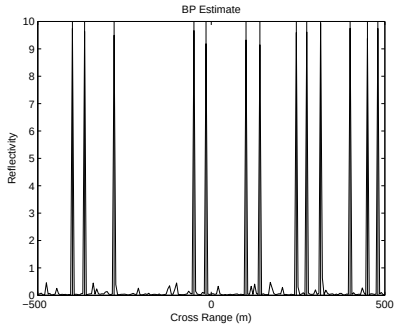

(a) $\nu = 1$

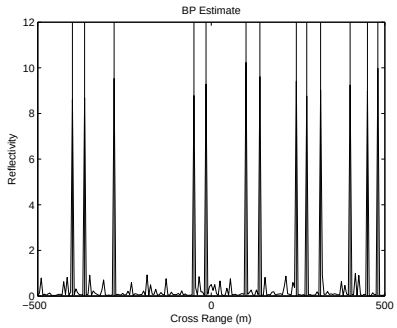

(b) $\nu = 3$

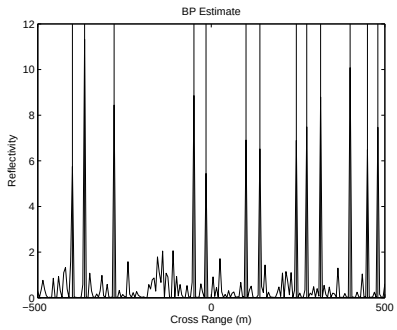

(c) $\nu = 5$

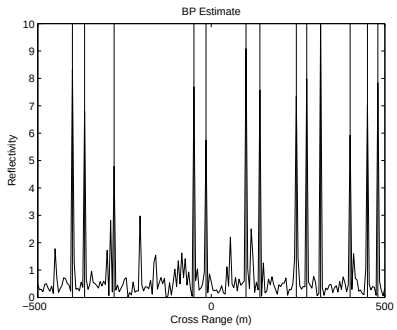

(d) $\nu = 10$

Figure II.2: BPDN simulation with increasing levels of measurement noise.

III

RADAR SIGNAL PROCESSING MODEL

III.1 Direct Scattering Problem for the Helmholtz Equation

Radar imaging utilizes the transmission of electromagnetic signals to gather information about a desired scene, as such the proper base for a model is Maxwell's equations [7, 15]. We also assume that electric field $\mathcal{E}$ is polarized

$$\mathcal{E}(x,t) = (0,0,E(x,t)), \quad x = (x_1, x_2) \in \mathbf{R}^2. \tag{III.1}$$

Then under appropriate assumptions on the background medium, E satisfies the scalar wave equation

$$\triangle E - \frac{1}{c^2(x)}\partial_t^2 E = 0 \tag{III.2}$$

where $c(x)$ is a function related to the medium inhomogeneities and $\triangle$ is the two dimensional Lalplacian operator

$$\triangle = \frac{\partial^2}{\partial x_1^2} + \frac{\partial^2}{\partial x_2^2}. \tag{III.3}$$

Here we consider time harmonic incident waves of the form

$$E(x,t) = \Re\left(u(x)e^{-i\omega t}\right). \tag{III.4}$$

Then u must satisfy the scalar Helmholtz equation

$$\triangle u + \frac{\omega^2}{c^2(x)}u = 0. \tag{III.5}$$

In the absence of scatterers and a homogeneous medium, the speed $c = c_0 = \text{const.}$ and the

incident field u^i satisfies the homogeneous equation

$$\triangle u^i + k^2 u^i = 0 \quad \text{in } \mathbf{R}^2 \tag{III.6}$$

where the wavenumber k is ω/c_0. In this case the imaging problem is trivial. We suppose that u^i propagates in an inhomogeneous medium characterized by a refractive index $n(x)$ with

$$n(x) := \frac{c_0^2}{c^2(x)}. \tag{III.7}$$

The inhomogeneities are assumed to be contained some ball B, hence $c = c_0$ outside of this ball and $1 - n(x)$ has compact support. The incident field is scattered by the inhomogeneities of the medium producing a scattered field u^s. The energy from u^s scatters outward so u^s satisfies the Sommerfeld radiation condition

$$\lim_{r\to\infty} |r|^{1/2} \left(\frac{\partial u^s}{\partial r} - ik u^s \right) = 0 \tag{III.8}$$

with $r = x/|x| \in S^1$.

Definition ([9]). *The **direct scattering problem** for the total field $u = u^i + u^s$ is*

$$\triangle u + k^2 n(x) u = 0 \tag{III.9}$$

$$u = u^i + u^s \tag{III.10}$$

where u^s satisfies the Sommerfeld radiation condition, and $k = \omega/c_0 > 0$.

III.2 The Inverse Scattering Problem

For notational convenience we set $v(x) := 1 - n(x)$ and note that v has compact support. We also suppose that n has nonnegative real and imaginary parts. The scattering problem for u is equivalent to the Lippman-Schwinger integral equation (Theorem 8.3 in [9])

$$u(x) = u^i(x) - k^2 \int \Phi(x, x')v(x')u(x')\, dx', \quad x \in \mathbf{R}^2 \tag{III.11}$$

where Φ is the fundamental solution to the Helmholtz equation. This is equivalent to the equation

$$u^s(x) = -k^2 \int \Phi(x, x')v(x')u(x')\, dx', \quad x \in \mathbf{R}^2 \tag{III.12}$$

for the scattered field. The Lippman-Schwinger equation combined with the Sommerfeld radiation condition implies that u^s has the far field asymptotic

$$u^s(x) = \frac{e^{ik|x|}}{|x|} A(\hat{x}) + O\left(\frac{1}{|x|^2}\right), \quad |x| \to \infty \tag{III.13}$$

with $\hat{x} = x/|x|$ on the unit sphere where A is the far field pattern given by

$$A(\hat{x}) = -\frac{k^2}{4\pi} \int e^{-ik\hat{x}\cdot x'} v(x')u(x')\, dx'. \tag{III.14}$$

The far field pattern will be the measured data of our scattering model. We apply the Born approximation and replace the total field u with u^i in the equation for A to get

$$A(\hat{x}) = -\frac{k^2}{4\pi} \int e^{-ik\hat{x}\cdot x'} v(x')u^i(x')\, dx'. \tag{III.15}$$

Definition ([9]). *The **inverse scattering problem** is to determine v from the knowledge of A by using III.15.*

Thus, the Born approximation linearizes the inverse problem for v since the total field is not

known in a neighborhood of the medium inhomogenities.

III.3 Signal Processing by Compressed Sensing

Traditional synthetic aperture radar signal processing is done by viewing the equation III.12 as an operator $T : \nu \mapsto u^s$ and applying an approximate inverse operator $T^* : u^s \mapsto \nu$ which preserves the singularities of ν, that is $\operatorname{sing\,supp} \nu \subset \operatorname{sing\,supp} T^* u^s$ [7, 1]. Krishnan et. al. [16] adopt a similar approach for multistatic synthetic aperture radar. The approach we adopt is to discretize the integral equation III.12 to obtain a linear system

$$Y = \Phi X \tag{III.16}$$

where Y is the data vector consisting of measurements of the far field pattern, Φ is the measurement matrix describing the geometry of data collection, and X is the discretized version of ν. We will focus on two different cases of ν: the scene consists of small targets so ν is a linear combination of delta functions, and the case where the scene consists of extended objects that can be approximated by a linear combination of step functions.

In the first case, the vector X will be sparse so the information determining X lies in only few of its entries. Developments in compressed sensing have shown that if X is s-sparse then the number of measurements required to determine X is of the same order as s, regardless if the actual dimension of X is large. Thus the dimension of the data Y can be much less than the dimension of X. A first guess at finding a sparse solution to III.16 is to find the sparsest solution by

$$\arg\min \|X\|_0 \quad \text{s.t.} \quad Y = \Phi X. \tag{III.17}$$

Note that $\|X\|_0$ is precisely the support of X. However, III.17 is a difficult combinatorial problem, in fact it is NP hard [4, 19]. To remedy this, Chen, Donoho, and Saunders [5] instead propose solving the ℓ^1 relaxtion called basis pursuit.

Definition. *The **basis pursuit** problem is*

$$\arg\min \|X\|_1 \quad s.t. \quad Y = \Phi X. \tag{III.18}$$

This is a convex optimization problem that is computationally contractible with many efficient implementations. We will present the main results guaranteeing the success of basis pursuit in obtaining the sparse solution to III.16, and in general, the success of basis pursuit is determined by properties of the sensing matrix Φ.

The first property we discuss is the null space property.

Definition. $\Phi \in \mathbf{C}_{n\times m}$ *satisfies the null space property (NSP) of order k with constant $\gamma \in (0,1)$ if*

$$\|\eta_T\|_1 \leq \gamma \|\eta_{T^c}\|_1 \tag{III.19}$$

for all sets $T \subset \{1,\ldots,m\}, \#T \leq k$ and for all $\eta \in \ker\Phi$ [13].

Here η_T denotes the restriction of η to the indices determined by T

$$(\eta_T)_j = \begin{cases} (\eta)_j & \text{if } j \in T, \\ 0 & \text{otherwise,} \end{cases} \tag{III.20}$$

and $T^c = \{1,\ldots,m\} - T$. We define

$$\sigma_k(X)_1 = \inf_{Z\in\Sigma_k} \|X - Z\|_1 \tag{III.21}$$

where the infimum is taken over all k-sparse vectors Z. This is simply the best k-sparse approximation to X as measured by the ℓ^1 norm. It is easy to see that $\sigma_k(X)_1 = \|X - X_{T^*}\|_1$ where T^* indexes the k entries of X having the largest moduli. The NSP yields the following performance guarantee for basis pursuit:

Theorem (Theorem 1 in [13]). *Let $n < m$ and let $\Phi \in \mathbf{C}_{n\times m}$ satisfy the NSP of order k with constant $\gamma \in (0,1)$. Let $X \in C^m$ and $Y = \Phi X$ and let $X^\#$ be a solution of the basis pursuit problem III.18. Then*

$$\|X - X^\#\|_1 \leq \frac{2(1+\gamma)}{1-\gamma}\sigma_k(X)_1. \tag{III.22}$$

In particular if X is k-sparse then $X^\# = X$.

Cohen, Dahmen, and DeVore proved that if all basis pursuit recovers all k-sparse X in $Y = \Phi X$, then Φ necessarily satisfies the NSP of order k with constant $\gamma \in (0,1)$ [8]. Hence the NSP of order k is equivalent to the success of basis pursuit in perfectly recovering k-sparse vectors.

A drawback of the NSP is that it is not easy to show directly, however the restricted isometry property (RIP) introduced by Tao and Candes [4] is easier to work with and establishes some performance guarantees as well.

Definition. *The restricted isometry constant of $\Phi \in \mathbf{C}_{n\times m}$ is the smallest number δ_k such that*

$$(1-\delta_k)\|Z\|_2^2 \leq \|\Phi Z\|_2^2 \leq (1+\delta_k)\|Z\|_2^2 \tag{III.23}$$

for all k-sparse vectors Z. Φ is said to satisfy the restricted isometry property of order k with constant δ_k if $\delta_k \in (0,1)$.

The RIP is in fact stronger than the NSP:

Theorem (Lemma 2 from [13]). *Suppose that $\Phi \in \mathbf{C}_{n\times m}$ satisfies the RIP of order $k+h =: K$ with constant $\delta_K \in (0,1)$. Then Φ has the NSP of order k with constant*

$$\gamma = \sqrt{\frac{k}{h}\frac{1+\delta_K}{1-\delta_K}}. \tag{III.24}$$

In particular, if Φ satisfies the RIP of order $3k$ with constant $\delta_{3k} < 1/3$ implies $\gamma < 1$ and consequently basis pursuit will recover all k-sparse vectors. Candes, Romberg, and Tao established in [3] that the RIP also guarantees the stability of recovery by basis pursuit when the measurements

are corrupted by noise. In this case $Y = \Phi X + E$ where E is exogenous noise. Exact recovery is, in general, not possible, so we look for a solution to a related problem called basis pursuit denoising:

$$\arg\min \|X\| \quad \text{s.t.} \quad \|\Phi X - Y\|_2 \leq \epsilon, \tag{III.25}$$

where $\epsilon > 0$ is a user parameter specifying the desired tolerance level.

Theorem (Theorem 1.1 in [3])**.** *Suppose that Φ satisfies the RIP of orders $3k$ and $4k$ with constants δ_{3k}, δ_{4k} respectively, and let $X^{\#}$ be a solution to the basis pursuit denoising problem III.25. Then if X is k-sparse and $\|E\|_2 \leq \epsilon$,*

$$\|X^{\#} - X\|_2 \leq C_k \epsilon \tag{III.26}$$

where the constant C_k depends only on δ_{4k}.

The role of the coherence of Φ was studied by Donoho and Elad in [10] and Gribonval in [14].

Definition. *The coherence of Φ, denoted $\mu(\Phi)$, is defined as*

$$\mu(\Phi) := \max_{i \neq j} \frac{|\sum_l \Phi_{jl} \Phi_{li}^*|}{\sqrt{\sum_l |\Phi_{li}|^2 \sum_l |\Phi_{lj}|^2}} \tag{III.27}$$

where Φ^* is the conjugate transpose of Φ.

The first result from [14] guarantees the success of basis pursuit provided that $\|X\|_0$ is small enough.

Theorem (Theorem 1 in [14])**.** *Let $n < m$ and let $\Phi \in \mathbf{C}_{n \times m}$ such that the columns of Φ span $\mathbf{C}^n$. If*

$$\|X\|_0 < \frac{1}{2}\left(1 + \frac{1}{\mu(\Phi)}\right) \tag{III.28}$$

then X is the unique solution to the ℓ^0 problem III.17 and the basis pursuit problem III.18.

Hence $\mu(\Phi)$ determines an upper bound on the sparsity of vectors that can be recovered via basis pursuit and smaller values of $\mu(\Phi)$ will permit the recovery of X even if X is not "sparse". The main advantage of the coherence approach is that $\mu(\Phi)$ can be computed directly.

A first immediate generalization of these results for sparse vectors X is the application to signals that are piecewise constant. Intuitively, such signals have sparse gradients; one first recovers the sparse gradient and the original signal can be obtained through integration. This approach is particularly useful when the signal X represents a two-dimensional image consisting of extended objects which are well approximated by a linear combination of step functions. Suppose that X is a piecewise constant one dimensional signal. Then the vector consisting of the forward differences of X is sparse. Candes, Romberg, and Tao proved in [2] that X can be recovered as the solution to

$$\arg\min \sum_j |X_{j+1} - X_j| \quad \text{s.t.} \quad \Phi X = Y. \tag{III.29}$$

This approach is especially useful in two dimensions, where two-dimensional images can be approximated by a linear combination of characteristic function of the unit square.

Definition ([2])**.** *Let g be a two-dimensional image represented by a matrix (g_{ij}). The **total variation norm** of g is defined as*

$$\|g\|_{TV} := \sum_{i,j} \sqrt{|D_1 g_{ij}|^2 + |D_2 g_{ij}|^2} \tag{III.30}$$

where D_1, D_2 are the forward difference operators

$$D_1 g_{ij} := g_{i+1,j} - g_{ij}, \quad D_2 g_{i,j} := g_{i,j+1} - g_{ij}. \tag{III.31}$$

*Let T be the linear measurement operator from the true image g to the measured data y. The **total variation minimization** problem is*

$$\arg\min \|g\|_{TV} \quad s.t. \quad y = Tg. \tag{III.32}$$

Candes et.al. proved [2] that TV-min III.32 is equivalent to III.18. In the case of noisy measurements $y = Tg + e$ where e is exogenous noise, Fannjiang in [11] proved performance guarantees

based on the RIP for **total variation denoising**

$$\arg\min \| f \|_{TV} \quad \text{s.t.} \quad \| Tg - f \|_2 \leq \epsilon. \tag{III.33}$$

for inverse scattering problems. In the following chapter, we demonstrate the application of basis pursuit and TV-min for two dimensional MIMO radar imaging based on the inverse scattering model presented.

IV

MIMO RADAR SIGNAL PROCESSING WITH COMPRESSED SENSING

IV.1 Point Targets and Basis Pursuit

Henceforth we regard the scattering problem in $\mathbf{R}^2$. We first consider the case where the medium consists of m point scatterers in a square lattice of spacing ℓ so that the scattering amplitude is

$$A(\hat{\mathbf{x}}, d) = \frac{\omega^2}{4\pi} \sum_{j=1}^{m} v_j u^i(\mathbf{x}_j) e^{-i\omega \mathbf{x}_j \cdot \hat{\mathbf{x}}} \tag{IV.1}$$

where $X = (v_j) \in \mathbf{C}^m$ is the target vector whose jth entry is the reflectivity of a point target at $\mathbf{x}_j$. We aim to establish performance guarantees on the performance of basis pursuit so that X can be recovered by solving

$$\min \|X\|_1 \quad \text{s.t} \quad \Phi X = Y \tag{IV.2}$$

where Φ is the sensing matrix consisting of array parameters dependent on the geometry of data collection, sampling rate, and signal type, and Y is vector of collected data. In our analysis we consider probing signals that are plane waves u_k^i with

$$u_k^i(\mathbf{x}) = e^{i\omega(x\cos\theta_k + y\sin\theta_k)}, \quad \mathbf{x} = (x, y) \in \mathbf{R}^2, \tag{IV.3}$$

each having incident direction determined by the angle θ_k and each having the same frequency. We suppose that the incident angles $\theta_k, k = 1, \ldots, n$ are i.i.d. uniform random variables on $[-\pi, \pi]$. We will consider the case where the transmit and receive arrays coincide, so if $\tilde{\theta}_k$ is a sampling angle we have $\tilde{\theta}_k = \theta_k + \pi$. Let Y_k be the vector of collected data due to the incident wave from transmitter k; the measured data is the scattering amplitude scaled by a factor of $(4\pi)/\omega)$. The

total data vector Y is formed by vertically stacking the Y_k's as

$$Y = \begin{pmatrix} Y_1 \\ \vdots \\ Y_n \end{pmatrix} \in \mathbf{C}^{n^2}. \tag{IV.4}$$

From this we can infer that the sensing matrix Φ has $(n(k-1)+l, j)$ entry given by

$$(\Phi)_{n(k-1)+l,j} = e^{[i\omega(x_j(\cos\theta_k+\cos\theta_l)+y_j(\sin\theta_k+\sin\theta_l))]} \tag{IV.5}$$

so that $\Phi \in \mathbf{C}^{n^2\times m}$. The dimension of the scene will typically be much greater than the dimension of the data, so the linear system $Y = \Phi X$ is underdetermined. Applying Fannjiang's results [12] to the present case, we obtain the following upper bound on the sensing matrix Φ: if

$$m \leq \frac{\delta}{8} e^{K^2/2} \tag{IV.6}$$

for some $\delta, K > 0$, then

$$\mu(\Phi) < \left(\frac{\sqrt{2}}{\sqrt{\pi\omega\ell}} + \frac{\sqrt{2}K}{\sqrt{n}}\right)^2 \tag{IV.7}$$

with probability greater than $(1-\delta)^2$. Then applying the coherence condition we conclude that with probability greater than $(1-\delta)^2$ BP perfectly reconstructs X if X is s-sparse and

$$s \leq \frac{1}{2} + \frac{1}{2}\left(\frac{n\sqrt{2}}{\sqrt{\pi\omega\ell}} + \frac{\sqrt{2}K}{\sqrt{n}}\right)^{-2}. \tag{IV.8}$$

IV.2 Piecewise Constant Targets

Here we consider the case where the target scene can be approximated by piecewise constant objects. In this case

$$\nu(x) = \sum_{j=1}^{m} \nu_j I\left(\frac{x}{\ell} - p_j\right) \tag{IV.9}$$

where I is the indicator function of the unit square $[-1/2, 1/2] \times [-1/2, 1/2]$ in $\mathbf{R}^2$ and p_j are points in the square lattice as in section IV.1. It is important to note that the scattering amplitude here is different than the case for a scene consisting of point targets that are clustered together. The scattering amplitude measured at sampling angle ϕ_l due to the kth incident probe is given by

$$\begin{aligned} A_k(\phi_l, \omega) = \ell^2 \frac{2\sin[(\omega\ell(\cos\theta_k - \cos\phi_l)]}{\omega\ell(\cos\theta_k - \cos\phi_l)} \frac{2\sin[(\omega\ell(\sin\theta_k - \sin\phi_l)]}{\omega\ell(\sin\theta_k - \sin\phi_l)} \\ \times \sum_p \nu_p e^{i\omega\ell(x_p(\cos\theta_k - \cos\phi_l) + y_p(\sin\theta_k - \sin\phi_l))} \end{aligned} \tag{IV.10}$$

where $\nu_p = \nu_j \Leftrightarrow p = p_j, j = 1, \ldots, m$ and $p = (x_p, y_p)$. We form the data vector as in the previous section; scale the $A'_k s$ by $4\pi/(\omega^2 g_{l,k})$ where

$$g_{l,k} = \frac{2\sin[(\omega\ell(\cos\theta_k - \cos\phi_l)]}{\omega\ell(\cos\theta_k - \cos\phi_l)} \frac{2\sin[(\omega\ell(\sin\theta_k - \sin\phi_l)]}{\omega\ell(\sin\theta_k - \sin\phi_l)} \tag{IV.11}$$

and set

$$Y = \begin{pmatrix} Y_1 \\ \vdots \\ Y_n \end{pmatrix} \in \mathbf{C}^{n^2} \tag{IV.12}$$

where each Y_k is the data collected due to the probe from θ_k. Then we define the sensing matrix Φ by having $(n(k-1) + l, j)$ entry

$$e^{i\omega\ell(x_j(\cos\theta_k - \cos\phi_l) + y_j(\sin\theta_k - \sin\phi_l))} \tag{IV.13}$$

where $p_j = (x_j, y_j)$ and the target vector X is defined by $(X)_j = \ell^2 \nu_{p_j}, j = 1, \ldots, m$. Then the inverse problem for ν can be posed as the underdetermined linear system

$$Y = \Phi X. \tag{IV.14}$$

The main difference between this sensing matrix and the matrix used for BP is the factor of ℓ in the argument of the exponential. From the results in [11] we conclude that TV-min can effectively recover X in the system (IV.14) for large enough n, but still with $n \ll m$. The success of TV-min is illustrated in section IV.3.

IV.3 Numerical Simulations

Figure IV.1 shows the reconstruction of a scene with 30 point targets using basis pursuit. For comparison, the least squares estimate is also shown. The parameter values are $\omega = 10, n = 20, \ell = 10, m = 2601$. In this case, BP has a high probability of exact reconstruction for the given level of sparsity. The BP implementation used is from Van Den Berg and Friedlander [22]. The results in figure IV.2 illustrate the failure of BP to accurately recover X when the sparsity exceed the admissible level determined by $\mu(\Phi)$. For this simulation, the sparsity was increased to 100 while leaving all other parameters fixed. The successful results of TV-min are given in figure IV.3. The same array parameter levels were used. The scene contains five extended two dimensional objects. The results in IV.4 illustrate the blurry reconstruction arising when the number of samples is reduced to $n = 10$. The implementation of TV-min used is by Li, et al.[17].

The previous simulations all neglect effects of exogenous noise. We can extend the model by supposing the measured data is corrupted by white noise as

$$Y = \Phi X + E. \tag{IV.15}$$

In this case we apply BP denoising for small targets and TV-min denoising for extended two dimensional targets. The results are shown in figures IV.5 and IV.6. The array parameters were the same as those used by

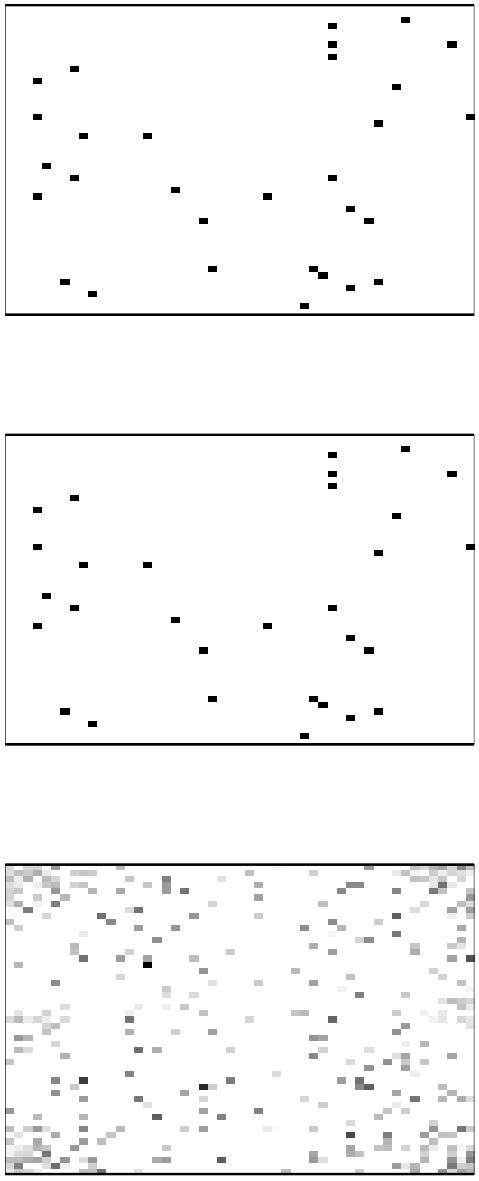

Figure IV.1: Scene reconstruction using basis pursuit with 30 point targets. The top is the actual scene, the middle is reconstruction using basis pursuit, and the bottom is the least squares approximation.

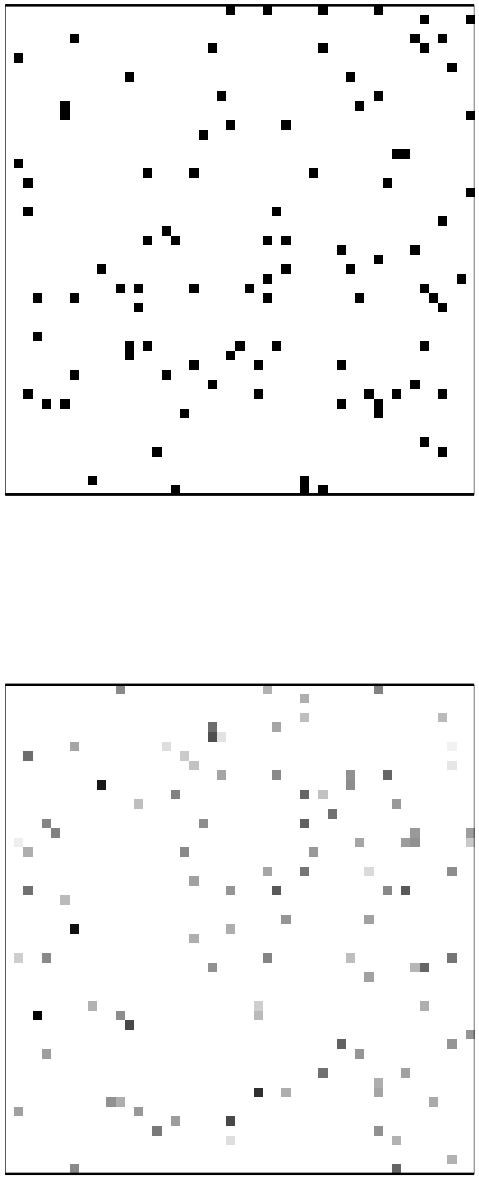

Figure IV.2: Scene reconstruction using basis pursuit with 100 point targets. The top is the actual scene and the bottom is the BP estimate. When the sparsity level exceeds the level permitted by $\mu(\Phi)$ BP fails to accurately recover X.

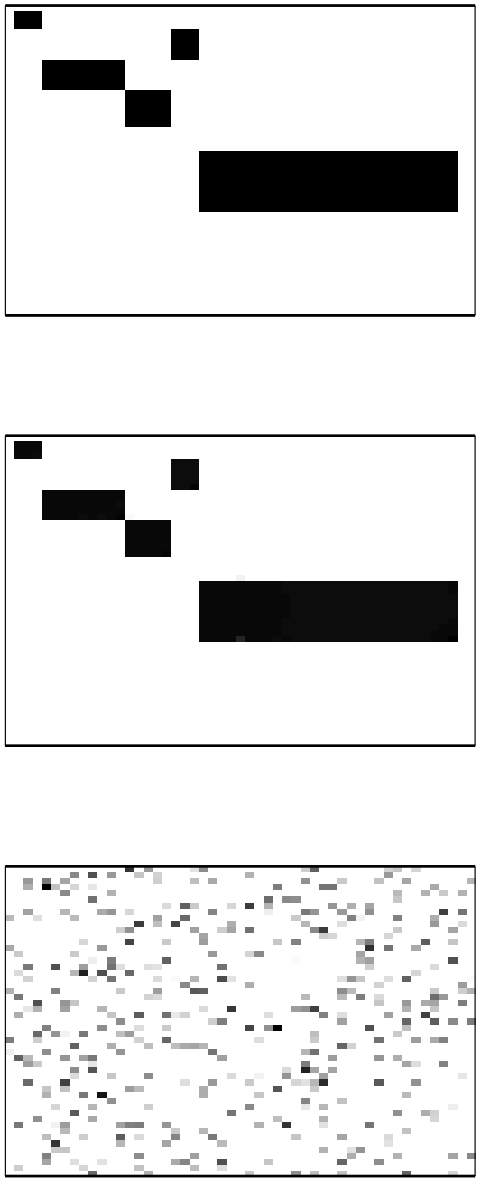

Figure IV.3: Scene reconstruction using TV-min with 5 piecewise constant objects. The top is the actual scene, the middle is reconstruction using TV-min, and the bottom is the least squares approximation.

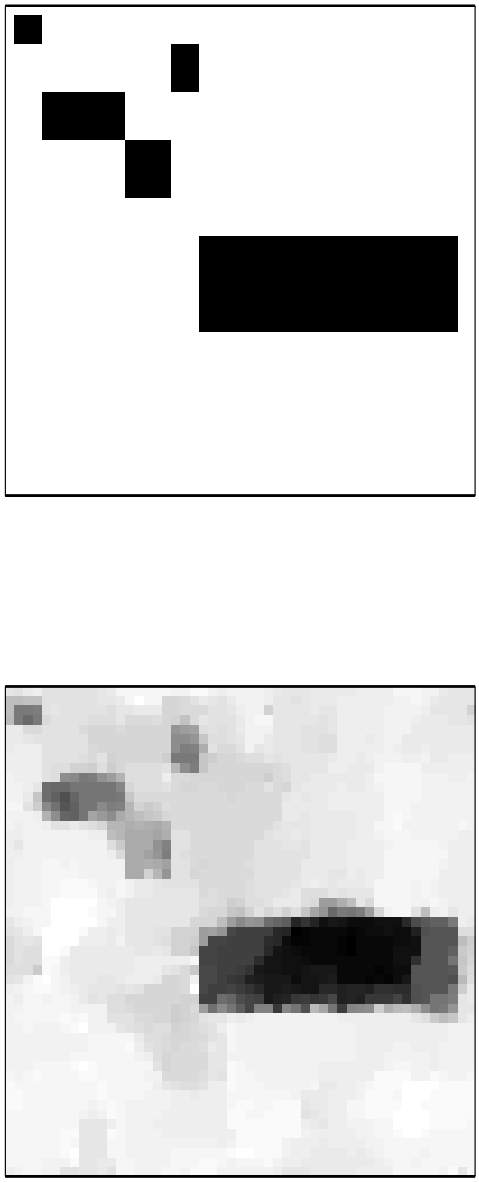

Figure IV.4: Blurry scene reconstruction using TV-min with 5 piecewise constant objects. The top is the actual scene and the bottom is the TV-min reconstruction.

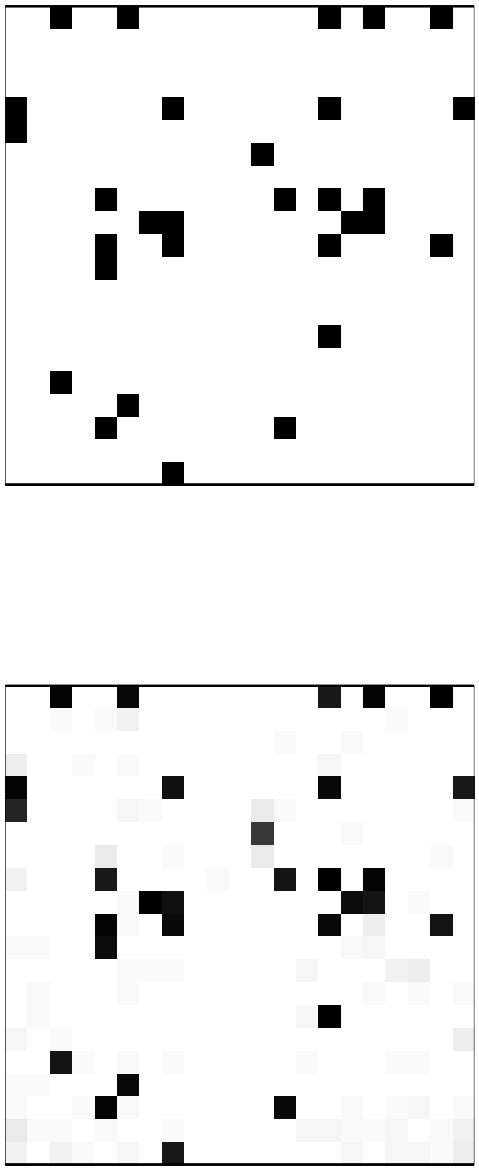

Figure IV.5: Basis pursuit denoising applied to noisy data. The top is the actual scene and the bottom is the BPDNs reconstruction.

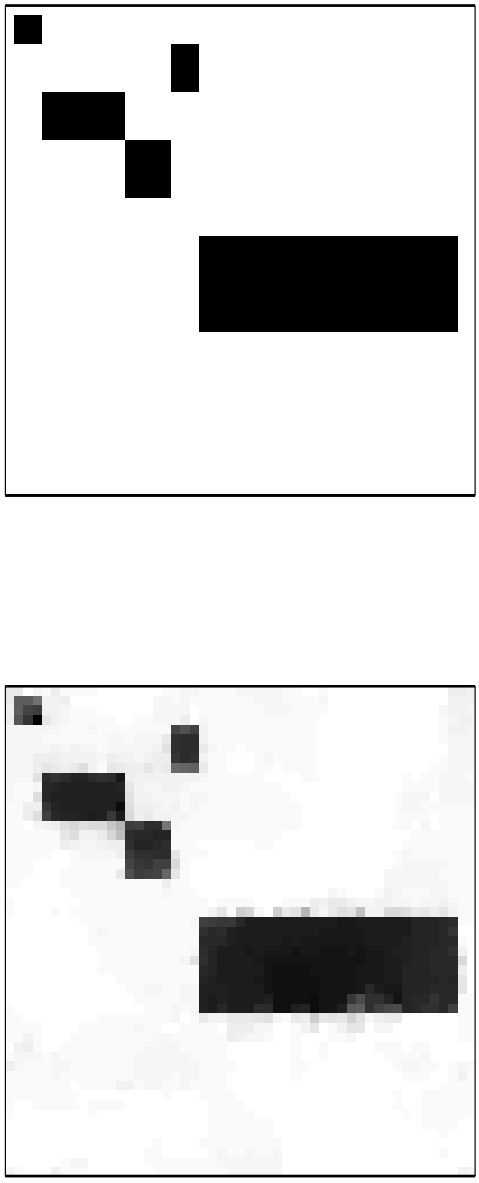

Figure IV.6: Scene reconstruction using TV-min denoising with 5 piecewise constant objects. The top is the actual scene, the middle is reconstruction using TV-min, and the bottom is the least squares approximation.

V

CONCLUSION

In this thesis we have presented positive results for the application of compressed sensing techniques in MIMO radar imaging. When compressed sensing techniques are applicable, they yield highly accurate reconstructions of the desired scene while utilizing few sampling resources. The results have a strong theoretical foundation being derived from an inverse scattering problem for the Helmholtz equation. It was shown that the sensing matrix in MIMO radar can be designed to yield positive results for using compressed sensing when the scene consists of small targets and extended two dimensional targets approximated by step functions.

BIBLIOGRAPHY

[1] Brett Borden. *Radar Imaging of Airborne Targets: A primer for applied mathematicians and physicists*. Taylor & Francis, 1999.

[2] Emmanuel J Candès, Justin Romberg, and Terence Tao. Robust uncertainty principles: Exact signal reconstruction from highly incomplete frequency information. *Information Theory, IEEE Transactions on*, 52(2):489–509, 2006.

[3] Emmanuel J Candes, Justin K Romberg, and Terence Tao. Stable signal recovery from incomplete and inaccurate measurements. *Communications on pure and applied mathematics*, 59(8):1207–1223, 2006.

[4] Emmanuel J Candes and Terence Tao. Decoding by linear programming. *Information Theory, IEEE Transactions on*, 51(12):4203–4215, 2005.

[5] Scott Shaobing Chen, David L Donoho, and Michael A Saunders. Atomic decomposition by basis pursuit. *SIAM journal on scientific computing*, 20(1):33–61, 1998.

[6] Scott Shaobing Chen, David L Donoho, and Michael A Saunders. Atomic decomposition by basis pursuit. *SIAM review*, 43(1):129–159, 2001.

[7] Margaret Cheney and Brett Borden. *Fundamentals of radar imaging*, volume 79. Siam, 2009.

[8] Albert Cohen, Wolfgang Dahmen, and Ronald DeVore. Compressed sensing and best k-term approximation. *Journal of the American Mathematical Society*, 22(1):211–231, 2009.

[9] David Colton and Rainer Kress. *Inverse acoustic and electromagnetic scattering theory*, volume 93. Springer, 2013.

[10] David L Donoho and Michael Elad. Optimally sparse representation in general (nonorthogonal) dictionaries via l1 minimization. *Proceedings of the National Academy of Sciences*, 100(5):2197–2202, 2003.

[11] Albert Fannjiang. Compressive inverse scattering with tv-min and greedy pursuit. *arXiv preprint arXiv:1205.3834*, 2012.

[12] Albert C Fannjiang. Compressive inverse scattering: I. high-frequency simo/miso and mimo measurements. *Inverse Problems*, 26(3):035008, 2010.

[13] Massimo Fornasier and Holger Rauhut. Compressive sensing. *Handbook of Mathematical Methods in Imaging*, 1:187–229, 2011.

[14] Rémi Gribonval and Morten Nielsen. Sparse representations in unions of bases. *Information Theory, IEEE Transactions on*, 49(12):3320–3325, 2003.

[15] David Jeffrey Griffiths and Reed College. *Introduction to electrodynamics*, volume 3. prentice Hall New Jersey, 1999.

[16] V Krishnan, J Swoboda, CE Yarman, and B Yazici. Multistatic synthetic aperture radar image formation. *Image Processing, IEEE Transactions on*, 19(5):1290–1306, 2010.

[17] Chengbo Li, Wotao Yin, and Yin Zhang. User's guide for tval3: TV minimization by augmented lagrangian and alternating direction algorithms. *CAAM Report*, 2009.

[18] Jian Li and Petre Stoica. *MIMO radar signal processing*. Wiley-IEEE Press, 2008.

[19] Balas Kausik Natarajan. Sparse approximate solutions to linear systems. *SIAM journal on computing*, 24(2):227–234, 1995.

[20] E. van den Berg and M. P. Friedlander. SPGL1: A solver for large-scale sparse reconstruction, June 2007. http://www.cs.ubc.ca/labs/scl/spgl1.

[21] E. van den Berg and M. P. Friedlander. Probing the pareto frontier for basis pursuit solutions. *SIAM Journal on Scientific Computing*, 31(2):890–912, 2008.

[22] E Van Den Berg and MP Friedlander. Spgl1: A solver for large-scale sparse reconstruction. *Online: http://www. cs. ubc. ca/labs/scl/spgl1*, 2007.

BIOGRAPHICAL SKETCH

Juan Francisco Lopez Jr. was born in McAllen, TX in 1989. He attended high school at McAllen High School in McAllen, TX. In 2011, he graduated with a B.S. in Mathematics from the University of Texas - Austin. He continued his education by earning his M.S. in Mathematical Sciences in 2013 from the University of Texas - Pan American. From 2011-2013, he worked on the "DoD Project on PDE Analysis and Radar Image Reconstruction". Juan has 2 papers published in the Proceedings of the 2012 and 2013 SPIE Defense, Security, and Sensing Conferences. He can be contacted at jflopezjr@outlook.com.